# Synthetic intracellular nanostructures enhance cytotoxic T cell function via assembly-driven chemical engineering

Sarah Chagri[1], Anna Burgstaller[2], Claudia Schirra[3], Julian Link[1], Zhixuan Zhou[4], Raphael Meyer[1], Jana Fetzer[1], Patrick Roth[1], Yong Ren[1], Shutian Si[1], Francesca Mazzotta[1], Manfred Wagner[1], Ingo Lieberwirth[1], Katharina Landfester[1], David Y.W. Ng[1,*], Oskar Staufer[2,*], Tanja Weil[1,*]

[1] Max Planck Institute for Polymer Research, 55128 Mainz, Germany

[2] Leibniz Institute for New Materials, 66123 Saarbrücken, Germany

[3] Cellular Neurophysiology, Center for Integrative Physiology and Molecular Medicine (CIPMM), Saarland University, 66421 Homburg, Germany

[4] State Key Laboratory of Chemo/Biosensing and Chemometrics, College of Chemistry and Chemical Engineering, Hunan University, Changsha, 410082 PR China

*Corresponding Authors: David Y.W. Ng, david.ng@mpip-mainz.mpg.de; Oskar Staufer, oskar.staufer@leibniz-inm.de; Tanja Weil, weil@mpip-mainz.mpg.de

## Abstract

Nature achieves diverse biological functions through structure formation. Inspired by the controlled formation of polypeptide nanostructures in cells, synthetic methods have been developed to assemble artificial nanostructures and organelle-like compartments within living cells. While these synthetic intracellular assemblies have mostly been used to disrupt cellular processes, their potential to induce a gain of function within cells remains unexplored. Here, we introduce redox-sensitive *iso*peptides that transform into self-assembling linear peptides inside human cytotoxic T cells in response to intracellular levels of glutathione. The *in situ* formation of synthetic peptide nanostructures in cytotoxic T cells leads to cellular stiffening, establishing a direct interface between biochemically driven peptide assembly and mechanobiological effects. This change in biophysical properties, along with increased phosphorylation of signaling proteins associated with T cell activation, correlates with a significant enhancement in the efficacy of cytotoxic T cells to eliminate cancer cells. Our findings elucidate the cellular impact of synthetic peptide nanostructures assembled within living cytotoxic T cells and demonstrate their ability to modulate and enhance effector immune cell responses.

## Introduction

Naturally occurring intracellular nanostructures, such as microtubules, actin filaments, and intermediate filaments that form the cytoskeleton, play a critical role in fundamental cellular processes, including metabolism, division and motility.[1] These complex, dynamic protein assemblies span the cytosol and provide a blueprint for the development of synthetic materials designed to form nanostructures in synthetic cells, a growing frontier in biomolecular engineering.[2] Moreover, the creation of synthetic architectures inside the complex environment of mammalian cells represents a significant milestone in nanomedicine and synthetic biology, providing a bottom-up approach that mimics natural intracellular assemblies and opens new avenues for supramolecular drug design.[3]

To date, advances in the creation of intracellular assemblies have primarily focused on the formation of synthetic nanostructures within cancerous cells with the goal of disrupting cellular metabolism and inducing apoptosis.[4,5] State-of-the-art strategies involve the use of bioresponsive molecules that can undergo chemical transformations in response to endogenous stimuli, enabling spatiotemporal control

and selectivity over the assembly formation.[3,6-10] However, these efforts to construct synthetic intracellular nanostructures have so far been limited to malignant cells[4,5], leaving the potential to modulate the behavior of non-cancerous cells, particularly immune cells, unexplored.

Our work explores a new direction in this field by harnessing synthetic intracellular nanostructures for the immunomodulation of cytotoxic T cells. Cytotoxic $CD8^+$ T cells play a crucial role in the immune response by directly targeting and eliminating cancerous or virus-infected cells.[11] The unmatched specificity of T cells in recognizing target cells is a key advantage in T cell-based therapies and their efficacy in inducing apoptosis is tightly linked to their activation status, which involves complex intracellular signaling pathways.[12] High cytotoxic effector function in T cells is desirable, as it enables a more robust and effective response against tumors, contributing to better therapeutic outcomes in adoptive cell therapy. The mechanical properties of T cells, such as stiffness and deformability, correlate with their activation and migration capabilities, as well as their ability to interact with target cells.[13] Enhancing the functional capacity of cytotoxic T cells by biochemical and biophysical means is therefore a central goal in immunotherapy.

In current clinical approaches, T cells are often modified outside the body through genetic engineering before being reinfused into the patient to combat cancer.[14,15] While ongoing efforts aim to enhance T cell efficacy by refining genetic engineering techniques, fewer strategies explore modulation of T cells through chemical engineering, for instance, via extracellular interactions with nanomaterials.[16-18] In our work, we propose a complementary strategy by intracellular chemical engineering: the *in situ* self-assembly of synthetic nanostructures within cytotoxic T cells to enhance T cell cytotoxicity. This approach holds the potential to further enhance T cell functionality beyond the limits of genetic modifications.

In T cells, glutathione, a reducing agent abundant in the cytosol[19], plays a critical role in maintaining redox homeostasis and facilitating metabolic reprogramming during T cell activation. It acts as an antioxidant to counterbalance the increased mitochondrial production of reactive oxygen species (ROS).[20-22] As ROS scavenging is essential for T cell activation, proliferation and effector function, activated T cells have been shown to contain significantly higher levels of intracellular glutathione compared to resting T cells.[21,23] Therefore, the glutathione-induced transformation of a bioresponsive assembly precursor within T cells is a promising strategy for the *in situ* generation of intracellular nanostructures that boost T cell activation dynamics and cytotoxic effector function against cancer cells. Shifting the focus from disrupting malignant cells to enhancing the beneficial functions of healthy cells, such as cytotoxic T cells, will be a next-generation technology for more sophisticated cell-material interactions. Modulating the behavior of these immune cells through *in situ*-formed artificial nanostructures would also have significant implications for immunotherapy.

Herein, we introduce glutathione-responsive *iso*peptides capable of undergoing a multistep reaction cascade upon cellular entry, resulting in the *in situ* formation of peptide nanostructures inside human cytotoxic T cells (Fig. 1). We report a significant stimulatory effect of these peptide nanostructures on cytotoxic T cell function, leading to enhanced cytotoxicity against breast cancer cells. Using confocal laser scanning microscopy (CLSM) and correlative light and electron microscopy (CLEM), we visualize the formation and localization of these nanostructures. Importantly, the enhancement of T cell effector function is directly correlated with intracellular nanostructure formation. Additionally, we examine activation of stimulatory T cell signaling of peptide-treated versus untreated T cells and evaluate the impact of synthetic intracellular nanostructures on T cell mechanical properties. This analysis aims to elucidate the biophysical and molecular mechanisms driving the observed functional enhancements. To our knowledge, this is the first study to demonstrate that synthetic intracellular nanostructures can

support and enhance beneficial cellular functions, offering a novel strategy to modulate immune cell responses.

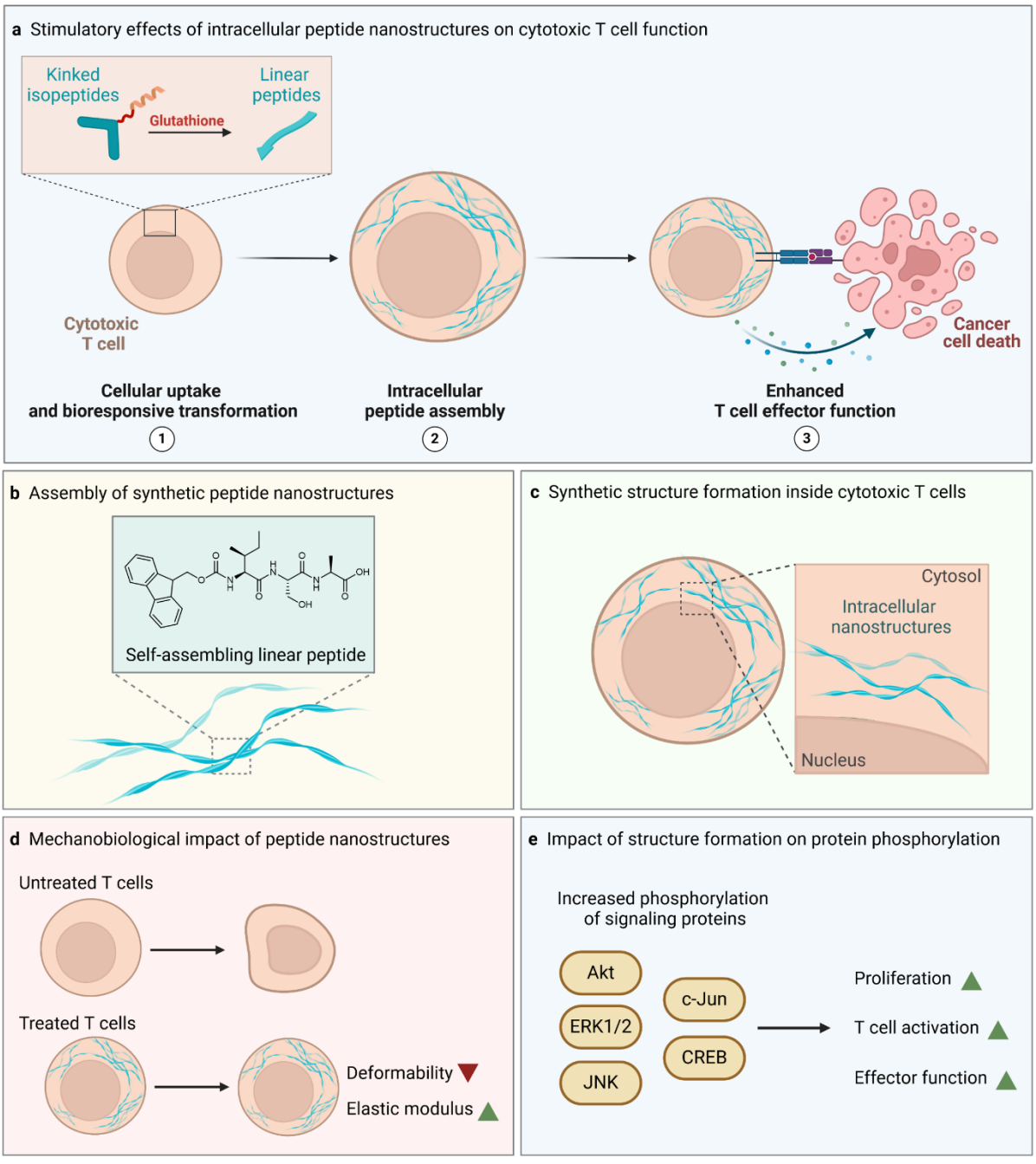


**Figure 1 Schematic overview of T cell engineering through intracellular synthetic nanostructures. a |** Glutathione-responsive kinked *iso*peptides undergo a bioresponsive transformation inside cytotoxic T cells, leading to the formation of linear, self-assembling peptides. This intracellular peptide assembly within human cytotoxic T cells enhances T cell-mediated cytotoxicity against cancer cells. **b |** The supramolecular properties and structural characteristics of the nanofiber-forming peptides were investigated. **c |** The *in situ* structure formation inside cytotoxic T cells was visualized using confocal laser scanning microscopy and correlative light and electron microscopy. **d |** Intracellular structure formation influences the mechanical properties of cytotoxic T cells, reducing their deformability and increasing the elastic modulus. **e |** Increased phosphorylation of key signaling proteins associated with T cell proliferation, activation, and effector function was observed following *in situ* nanostructure formation.

## Results

### Design, synthesis and transformation of glutathione-responsive *iso*peptides

The glutathione-responsive *iso*peptide **1a**, along with the control *iso*peptide **1b**, consists of three key structural components: (1) the cell-penetrating peptide sequence TAT (transactivator of transcription) derived from human immunodeficiency virus (HIV), (2) a glutathione-responsive trigger group that can undergo reductive degradation and (3) the kinked *iso*peptide with an aromatic *N*-terminal group (Fig. 2a). This *N*-terminal group either promotes supramolecular assembly (Fmoc in **1a**) or prevents assembly of the linear product (NBD in **1b**) resulting from the glutathione-triggered transformation (Fig. 2a).

The synthesis of the kinked *iso*peptides **1a** and **1b** was achieved through a combination of solid-phase peptide synthesis and solution-phase synthesis (Scheme S1). To analyze the glutathione-induced transformation of the *iso*peptides (Fig. 2b), we investigated the kinetics of this multistep reaction cascade (Fig. 2b) using liquid chromatography-mass spectrometry (LC-MS) (Fig. 2c). By analyzing the *m/z* values of the emerging peaks in the LC traces, we identified and assigned the reactive intermediates and final products of the glutathione-induced conversion (Fig. 2c,d).

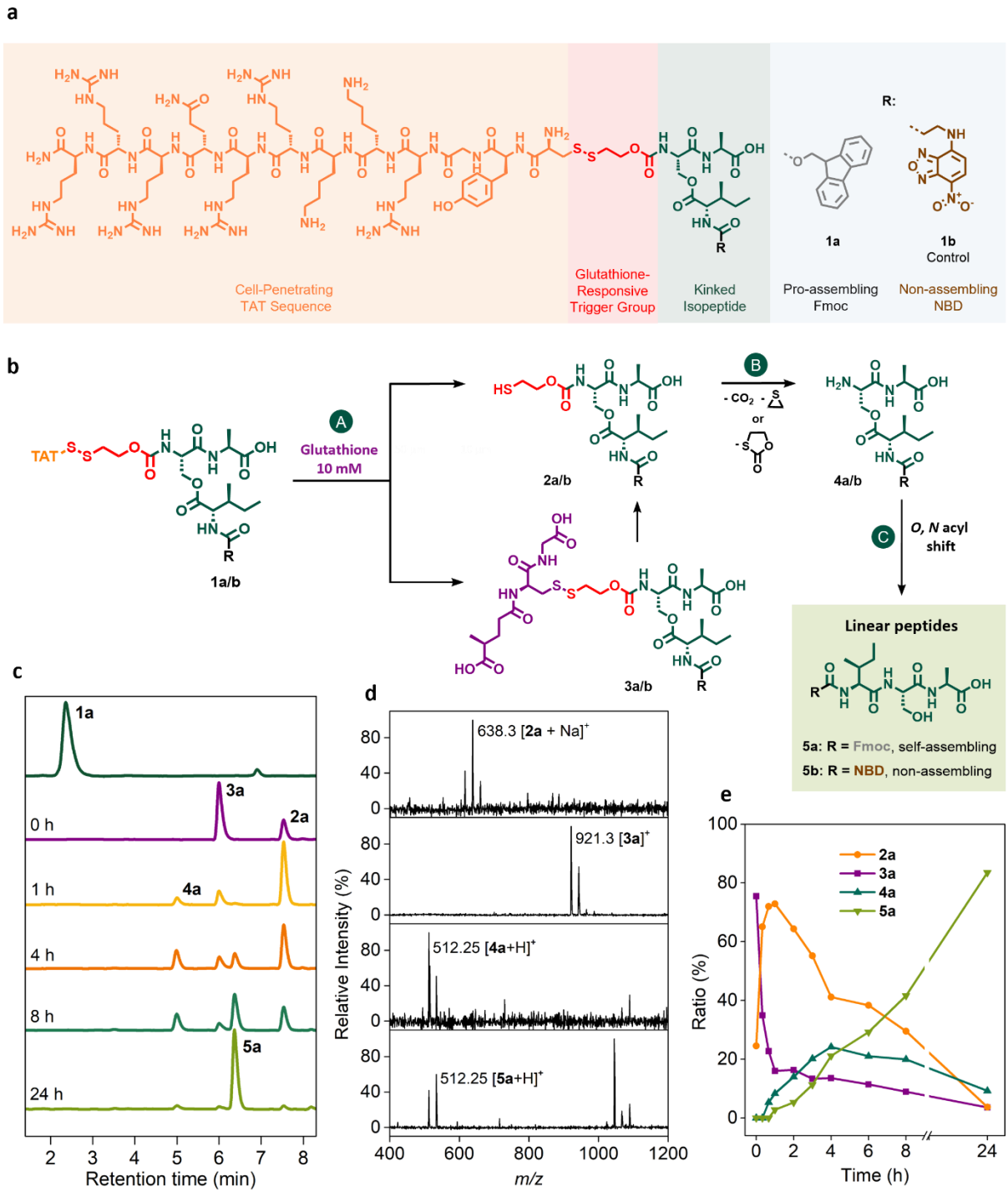


**Figure 2 Chemical structure and multistep conversion of glutathione-responsive *iso*peptides. a|** Chemical structures of glutathione-responsive *iso*peptides **1a** (with a Fmoc (9-fluorenylmethoxycarbonyl) group) and **1b** (with an NBD (nitrobenzodiazole) unit). **b|** Reaction scheme illustrating the multistep conversion of pro-assembling *iso*peptides **1a** or the control *iso*peptide **1b** into the self-assembling linear peptide **5a** or the non-assembling linear peptide **5b**. **c |** LC-MS kinetic analysis of the glutathione-induced linearization of **1a** in $NH_4HCO_3$ buffer (50 mM, pH 7.4) and methanol (v/v 1:1) in the presence of intracellular concentrations of glutathione (reduced glutathione: 10 mM; oxidized glutathione: 1 mM) at room temperature. **d |** Convoluted MS spectra identifying the intermediates **2a** ($t_R$ = 7.53 min), **3a** ($t_R$ = 6.00 min) and **4a** ($t_R$ = 4.98 min) as well as the final linear peptide **5a** ($t_R$ = 6.37 min) during the LC-MS analysis. **e |** Molar ratio of intermediates **2a**, **3a**, **4a** and final product **5a** after the addition of glutathione-containing buffer, based on the peak integration at 254 nm.

In the presence of intracellular levels of glutathione (reduced glutathione: 10 mM; oxidized glutathione: 1 mM)[24] in $NH_4HCO_3$ buffer (50 mM, pH 7.4), *iso*peptide **1a** underwent instant degradation, so that upon the first LC-MS injection, its signal ($t_R$ = 2.36 min) was no longer detectable

(Fig. 2c). Instead, two cleavage products, **2a** ($t_R$ = 7.53 min) and **3a** ($t_R$ = 6.00 min), were identified. These two intermediate products result from the nucleophilic attack of glutathione on the disulfide bond of **1a**, occurring at either of the two sulfur atoms (Fig. 2b). As the disulfide bond of the glutathione adduct **3a** is similarly susceptible to reductive cleavage, the transformation of **3a** also gave rise to the *iso*peptide with a free thiol group **2a** over time. After one hour, the unprotected *iso*peptide **4a** ($t_R$ = 4.98 min) was detected as the product of the self-immolation of the trigger group (Fig. 2c). The subsequent *O,N* acyl shift caused the linearization of **4a**, indicated by the increasing peak corresponding to the linear peptide **5a** ($t_R$ = 6.37 min). After 24 h, the linear self-assembling Fmoc-ISA **5a** became the most prominent peak in the LC trace (Fig. 2c), reflecting a conversion of 84% of the initial *iso*peptide **1a** into the self-assembling linear monomer **5a** (Fig. 2e).

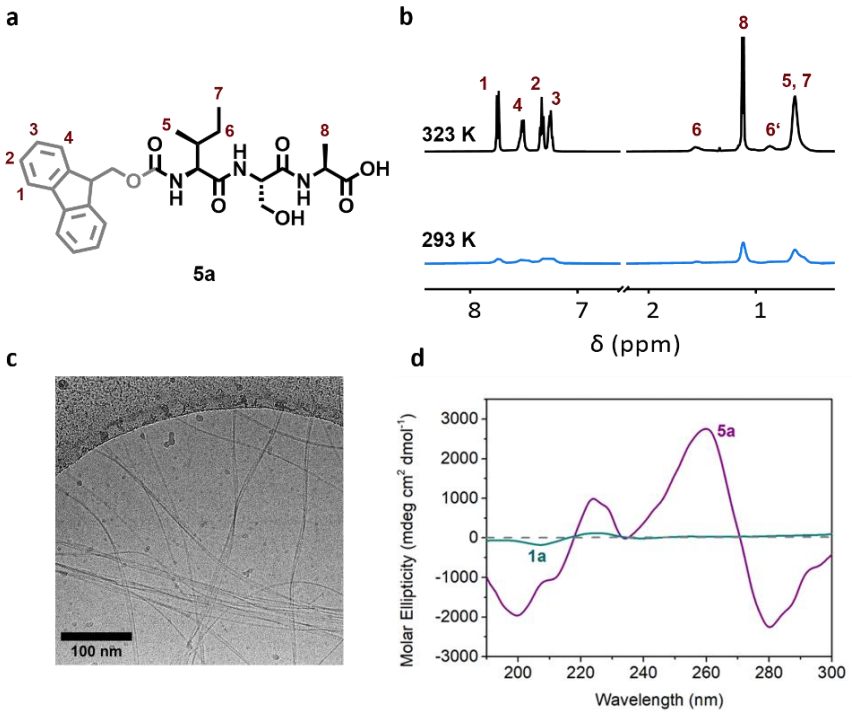


**Figure 3 Supramolecular assembly of linear peptide. a |** Chemical structure of **5a** with labeled protons. **b |** $^1$H NMR analysis of self-assembly behavior of **5a** (1 mg/ml) in deuterated phosphate buffer (50 mM) and DMSO-$d_6$ (9:1) at 293 K and 323 K. **c |** Cryo-TEM image of peptide nanofibers formed by linear peptide **5a** (1 mg/ml) in Dulbecco's phosphate buffered saline (DPBS) (pH 7.4) and DMSO (99:1). Scale bar 100 nm. **d |** Circular dichroism spectra of linear peptide **5a** and *iso*peptide **1a** (500 µM each) in phosphate buffer (10 mM, pH 7.4). The spectrum of **5a** shows characteristic signals of attractive peptide backbone interactions and aromatic interactions between Fmoc groups, while the spectrum of **1a** shows no signals indicating chirality.

The supramolecular assembly behavior of the linear peptide **5a** was analyzed using nuclear magnetic resonance (NMR) spectroscopy, circular dichroism (CD) spectroscopy, transmission electron microscopy (TEM) and cryogenic transmission electron microscopy (cryo-TEM) (Fig. 3).

Temperature-dependent $^1$H NMR spectroscopy of the linear peptide **5a** revealed significant peak broadening at room temperature (293 K), which is characteristic of supramolecular interactions between peptide monomers in aqueous solution (deuterated phosphate buffer (50 mM) and DMSO-$d_6$ (9:1)) (Fig. 3b and Fig. S21). Upon heating the solution to 323 K, sharp signals corresponding to the aromatic Fmoc head group and side chain groups of peptide **5a** emerged (Fig. 3a,b), indicating a higher amount of detectable monomeric peptide **5a** in solution at elevated temperatures.

CD spectroscopy was used to further characterize the secondary structure of linear Fmoc-ISA **5a** and kinked *iso*peptide **1a** (Fig. 3d). The CD spectrum revealed a nanoscale chirality of the self-assembling peptide **5a**, which arises from the chiral arrangement of the peptide monomers within the assembled

nanostructure.[25] The spectrum of **5a** displays a maximum at 260 nm that is characteristic for the π → π* transitions of the aromatic Fmoc groups[26]. Additionally, another maximum was observed at 224 nm indicating a n → π* transition of the carbonyl groups in the peptide backbone due to hydrogen bonding.[27,28] In contrast, the non-assembling kinked *iso*peptide **1a** showed no discernable chirality of the secondary structure, underlining the necessity of the transformation from kinked **1a** to linear **5a** to achieve the desired supramolecular interaction required for structure formation (Fig. 3d).

Dry-state TEM images of the linear peptide **5a** revealed its ability to self-assemble into long nanofibers in Dulbecco's phosphate buffered saline (DPBS) with 1% DMSO (Fig. S23). To investigate the impact of incorporating another linear peptide modified with a fluorophore, which is crucial for detecting nanostructures inside living cells, we studied the co-assembly of fluorescent Coumarin343-functionalized peptide **5c** with **5a** in a 5:1 ratio. TEM images confirmed that the presence of peptide **5c** did not disrupt nanofiber formation (Fig. S24). Similarly, when Cyanine5 (Cy5)-functionalized peptide **5d** was co-assembled with peptide **5a** at a 99:1 ratio, the nanofiber integrity was preserved. In contrast, co-assembly of the kinked assembly precursors **1a** and **1c** (Coumarin343-modified) (5:1 ratio) or **1a** and **1d** (Cy5-modified) (99:1 ratio) did not produce any observable superstructures (Fig. S24), emphasizing again the importance of the glutathione-induced linearization to induce self-assembly. Additionally, the more hydrophilic nitrobenzodiazole (NBD)-modified control *iso*peptide **1b** and its corresponding linear peptide **5b** also did not form any nanostructures, which allows evaluating cellular uptake and glutathione-induced rearrangement without subsequent peptide assembly (Fig. S24).

Cryo-TEM provided further insights into the peptide nanostructures of the Fmoc-functionalized peptide **5a** in an aqueous environment (DPBS with 1% DMSO). Consistent with dry-state TEM, cryo-TEM images revealed long, thin nanofibers of linear peptide **5a** with a slightly twisted morphology (Fig. 3c and Fig. S25 and S26). The twisted fibers exhibited an average thickness of 6.8±0.3 nm at the twists and 11.0±0.2 nm at the non-twisted regions (Fig. S26). The critical aggregation concentration (CAC) of the linear peptides was determined via a Proteostat aggregation assay, which is a fluorescence-based technique used to detect β-sheet driven assembly formation. The CAC for linear peptide **5a** in DPBS with 1% DMSO was found to be 10 µM (Fig. S27). For the co-assemblies with either the Coumarin343-containing linear peptide **5c** (5:1 ratio) or the Cy5-modified linear peptide **5d** (99:1 ratio), the CAC was 9.2 µM and 4.6 µM, respectively (Fig. S27). These results further confirm that the incorporation of fluorescent monomers **5c** or **5d** does not hinder nanostructure formation.

In summary, our analysis demonstrates that the multistep conversion of kinked *iso*peptide **1a** into the linear self-assembling peptide **5a** can be effectively triggered by physiological levels of glutathione. Physicochemical characterization of linear peptide **5a** further reveals its ability to form peptide nanofibers at low micromolar concentrations, highlighting its potential for the *in situ* formation of synthetic nanostructures in the intracellular environment.

## Cellular uptake and *in situ* formation of peptide nanostructures in T cells

Next, we explored the glutathione-induced conversion of the *iso*peptides into the corresponding linear peptides and subsequent nanostructure formation within cytotoxic T cells. First, primary human $CD8^+$ T cells were activated *ex vivo* by isolating them from healthy donors and co-incubating with anti-CD3/CD28 activation beads. This cross-linking of CD3 and CD28 receptors, combined with interleukin 2 (IL-2), induces T cell activation into an effector state and promotes polyclonal expansion.

We then investigated the uptake and co-assembly of the pro-assembling *iso*peptide **1a** together with a fluorescently labeled *iso*peptide (either **1c** with Coumarin343 or **1d** with Cy5) in these *ex vivo* expanded cytotoxic T cells (Fig. 4). CLSM of activated T cells treated with the *iso*peptides **1a:1c** (5:1) at 5 µM for 1 hour revealed the formation of fluorescent peptide nanostructures in the cytosol, the

nucleus and in the perinuclear region, also visible as high-contrast regions in the brightfield images (Fig. 4a).

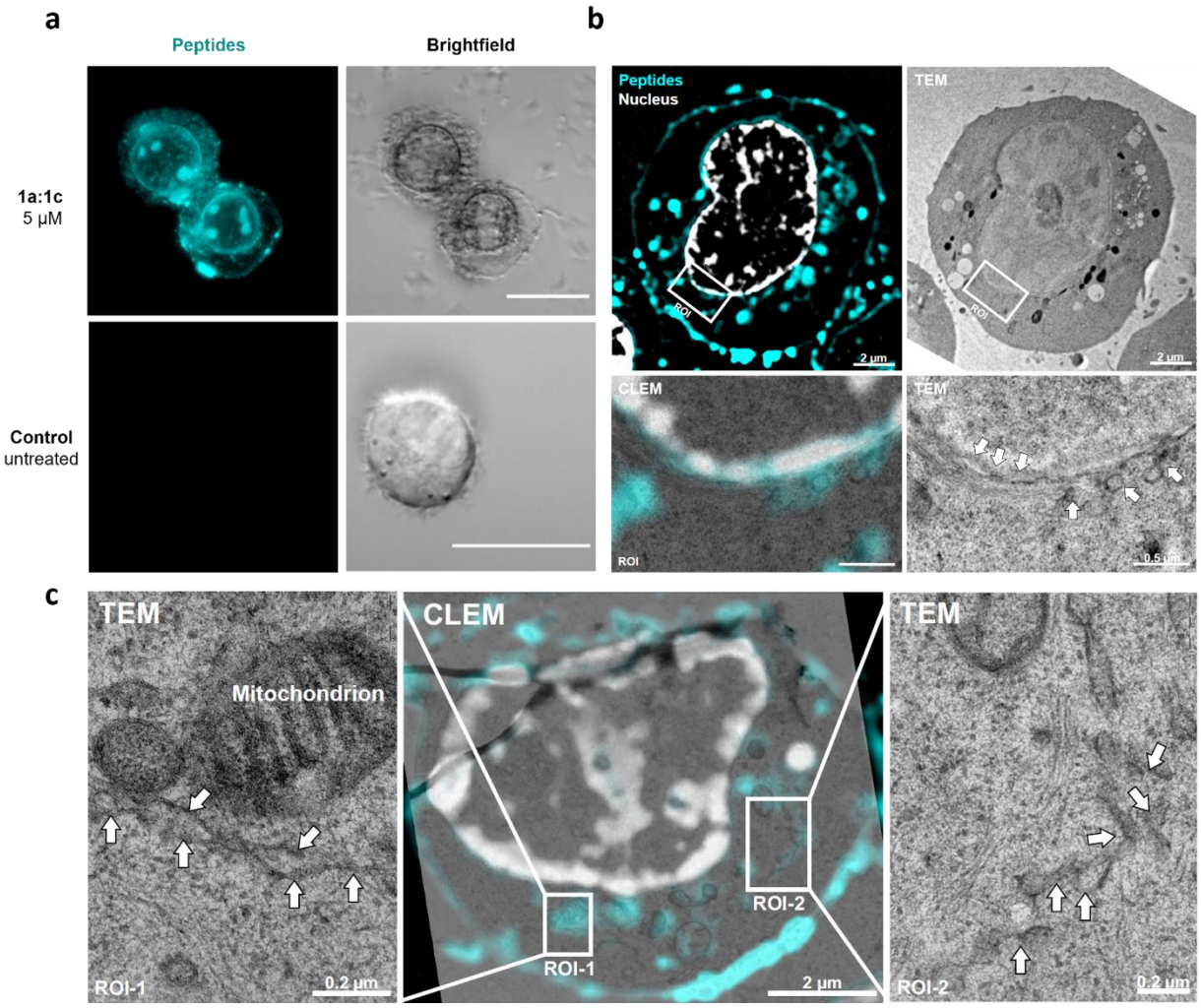


**Figure 4 Cellular uptake and intracellular peptide nanostructure formation in cytotoxic T cells. a |** Confocal laser scanning microscopy (CLSM) images of activated T cells incubated with 5 µM of glutathione-responsive *iso*peptides **1a** and **1c** (5:1) (cyan) for 1 hour, demonstrating the formation of intracellular peptide nanostructures in the cytosol and perinuclear region. Untreated T cells served as controls. Scale bar: 15 µm. **b** | Correlative light and electron microscopy (CLEM) images of activated human $CD8^+$ T cells treated with 5 µM of glutathione-responsive *iso*peptides **1a** and **1d** (99:1) (cyan) for 1 hour before freezing, highlighting the formation of fluorescent peptide nanostructures at the nuclear membrane and perinuclear region. **c** | CLEM images focusing on the localization of peptide nanostructures within the cytosol. The integrity of subcellular compartments of T cells appear unaffected by intracellular structure formation.

Further validation of in situ peptide assembly was conducted using CLEM (Fig. 4b,c). Pre-activated and *ex vivo* expanded cytotoxic T cells treated with *iso*peptides **1a:1d** (99:1) were analyzed, with Cy5-labeled *iso*peptide **1d** selected for co-assembly due to its superior fluorescence properties. CLEM images revealed fluorescent nanostructures distributed throughout the cytosol, perinuclear region, and at the cell membrane (Fig. 4b,c). The observed fiber thickness ranged from approximately 3.5 to 7.5 nm, consistent with the cryo-EM findings for peptide nanofibers in buffered solution (see Fig. 3c). Importantly, despite the widespread presence of peptide nanostructures within the cytosol and near the nucleus, the overall integrity of the T cells, including organelles such as mitochondria, remained intact (Fig. 4b,c). This indicates that incubation with *iso*peptides **1a:1d** at 5 µM for 1 hour did not significantly disrupt cellular or subcellular structures. These results underscore that the self-assembly of peptides at low concentrations does not compromise the cellular integrity of activated T cells.

In contrast, activated T cells treated with the NBD-functionalized control *iso*peptide **1b** at 5 µM for 1 hour exhibited no nanostructure formation and lower intracellular fluorescence (Fig. S34), reflecting the lack of self-assembling capability of the linear NBD-modified peptide **5b** (Fig. S24). Cellular uptake analysis of resting, i.e. non-activated, T cells treated with the pro-assembling *iso*peptides **1a:1d** (99:1) at 5 µM for 1 hour showed markedly lower intracellular fluorescence compared to activated T cells treated with the same peptides (Fig. S35). This aligns with the observation that fiber assembly is glutathione-dependent and activated T cells have reportedly higher cytosolic glutathione levels.[21,23]

## Functional impact of intracellular peptide nanostructures on cytotoxic T cells

Next, we examined how the synthetic intracellular peptide nanostructures impact the morphology and immunological function of cytotoxic T cells, specifically their ability to eliminate cancer cells. To evaluate the cytotoxicity of *ex vivo* pre-activated $CD8^+$ T cells against MCF-7 breast cancer cells, we combined the cytotoxic T cells with a bispecific T cell engager (BiTE) – a dual-targeting antibody that binds both the CD3 complex on T cells and the Human Epidermal Growth Factor Receptor 2 (HER2) on MCF-7 cells – followed by a 24-hour co-culture incubation with the cancer cells.

Treatment of cytotoxic T cells with glutathione-responsive *iso*peptides **1a:1c** (5:1, 5 µM) for 1 hour prior to the addition of BiTE and co-culturing significantly enhanced their cytotoxicity against the cancer cells. T cells pre-treated with these *iso*peptides exhibited a markedly lower $IC_{50}$ value for the bispecific T cell engager of 0.34 pM compared to 3.81 pM in untreated control T cells (Fig. 5a,b). Similarly, the use of *iso*peptides **1a:1d** (99:1, 5 µM), which includes the Cy5-labeled peptide used also for CLEM analysis, yielded comparable enhancements in cytotoxicity, indicating that the choice of fluorescent label does not impact the functional efficacy of the synthetic peptide nanostructures (Fig. S31). In contrast, T cells pre-treated with control *iso*peptide **1b**, which is internalized but only releases a linear NBD-modified peptide incapable of forming intracellular nanostructures, did not exhibit increased cytotoxicity (Fig. S30). These findings suggest that the observed enhancement in cytotoxicity is due to the formation of synthetic intracellular peptide nanostructures.

Towards revealing the functional mechanism behind the increased cytotoxic effect, we analyzed the rheological changes in T cells treated with pro-assembling *iso*peptides *via* single cell real-time deformation cytometry (RT-DC). T cell activation and adhesion to the antigen presenting cells (in this case the HER2-presenting MCF7 breast cancer cells) is greatly influenced by the mechanical properties of the T cells, which in turn are governed by cytoskeletal tensions and acto-myosin contractions.[29] Both the actin and microtubule cytoskeleton play crucial roles in establishing T cell polarity, migration, formation of the immunological synapse and the directed secretion of cytokines and cytolytic granules.[30] RT-DC measurements revealed that T cells treated with *iso*peptides **1a:1c** for 1 h at 5 µM exhibited notable changes in morphology and stiffness (Fig. 5c,d,e). Specifically, these T cells demonstrated significantly reduced deformability (Fig. 5c) and an increased elastic modulus (Fig. 5d) compared to the untreated controls. This indicates a general stiffening of the activated T cells that results from the presence of synthetic intracellular nanostructures.

To elucidate the downstream signaling effects of peptide nanostructures within T cells, we correlated enhanced T cell effector functions and mechanobiological changes with alterations in signaling protein phosphorylation by a Phospho-Kinase Antibody Arrays (Fig. 5f and Fig. S32). We observed significant changes in the phosphorylation of key signaling proteins, including Akt, c-Jun, CREB, ERK1/2 and JNK, in cytotoxic T cells treated with pro-assembling *iso*peptides **1a:1c** (Fig. 5f). These proteins are integral components of pathways that drive T cell activation, proliferation and effector function. Elevated phosphorylation of Akt, a central kinase in the PI3K/Akt pathway,[31] suggests enhanced survival, along with elevated expression of key adhesion and cytolytic molecules in T cells.[32-34] The increased phosphorylation of c-Jun, a member of the activator protein-1 (AP-1) family, further promotes the

expression of genes required for T cell activation and proliferation.[35,36] Similarly, the higher levels of phosphorylated transcription factor CREB were found in peptide-treated T cells, indicating activation of gene expression essential for T cell effector function and cytokine production.[37] The elevated phosphorylation levels of ERK1/2 and JNK, which are key mitogen-activated protein (MAP) kinases, further support the notion of heightened T cell proliferation and effector function.[38-40] In contrast, T cells treated with the non-assembling control *iso*peptide **1c**, which can enter cells and undergo glutathione-induced transformation but lacks the ability to form assemblies, did not exhibit increased phosphorylation of these proteins (Fig. S32). This finding highlights that the observed effects on signaling proteins are specifically associated with the formation of synthetic peptide nanostructures within T cells.

Collectively, these findings demonstrate that the glutathione-triggered formation of peptide nanostructures not only alters the mechanobiological properties of T cells but also potentiates intracellular signaling pathways linked to an enhanced T cell immune response.

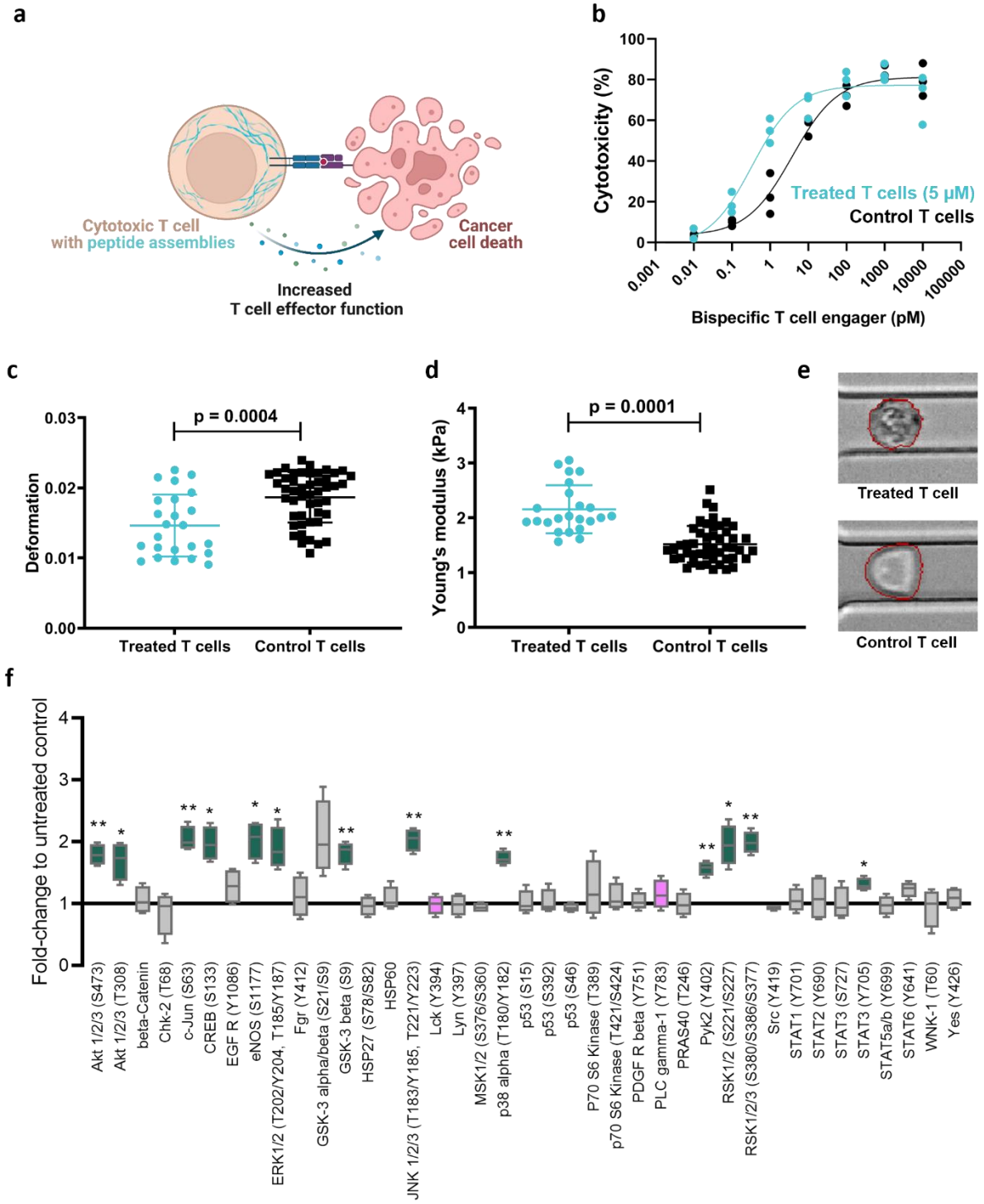


**Figure 5 Enhancement of T cell cytotoxicity against MCF-7 cancer cells and alterations in mechanobiology and protein phosphorylation by intracellular peptide nanostructures. a** | Schematic illustration of the co-stimulation of T cell cytotoxicity via intracellular peptide assembly. **b** | Dose-response curve showing the cytotoxic effect of activated T cells against HER2-expressing MCF7 cancer cells in relation to the concentration of a bispecific T cell engager targeting HER2 and CD3. The black curve represents data for untreated T cells, while the blue curve shows data for T cells pre-treated with the *iso*peptides **1a:1c** (5:1) at 5 µM for 1 hour, followed by washing and addition of the bispecific engager (n = 3 donors, mean of 2 technical replicates each). The $IC_{50}$ of the bispecific engager for untreated T cells is 3.81 pM, compared to 0.34 pM for *iso*peptide-treated cells. **c** | Real-time deformability cytometry (RT-DC) analysis showing reduced deformation in T cells pre-treated with the *iso*peptide mixture **1a:1b** (5:1) at 5 µM for 1 hour, relative to untreated controls. **d** | RT-DC measurements indicating an increased Young's modulus in T cells treated with the *iso*peptide mixture, reflecting enhanced cellular stiffness. **e** | Brightfield images of treated (**1a:1b** (5:1) at 5 µM for 1 hour) and untreated control T cells during RT-DC measurements within a microfluidic channel. **f** | Proteome Profiler Human Phospho-Kinase Antibody Array analysis of T cells treated with the

*iso*peptides **1a:1c** (5:1) at 5 µM for 1 hour (n = 2 donors, 2 on-membrane replicates), highlighting differential phosphorylation in a panel of key signaling proteins essential for T cell activation.

## Conclusion

In this study, we have demonstrated the chemical engineering of activated human cytotoxic T cells through the *in situ* formation of intracellular synthetic peptide nanofibers that alter critical T cell functions, ultimately improving the immune response against cancer cells. By using redox-sensitive *iso*peptides, we successfully induced the assembly of synthetic nanostructures within the intracellular environment of cytotoxic T cells, resulting in a significant boost to their cytotoxic effector function. The formation of these peptide nanostructures not only altered the mechanical properties of the T cells, leading to increased stiffness and decreased deformability, but also promoted central signaling pathways involved in the activation and regulation of T cells. This dual impact on both the physical and biochemical attributes of T cells underscores the potential of intracellular nanostructures as a tool for modulating immune cell behavior beyond genetic engineering. By focusing on augmenting the intrinsic functions of healthy immune cells, this work could pave the way for innovations in the field of immunotherapy. The ability to fine-tune immune cell properties through controlled intracellular assembly could potentially open up new possibilities for the design of next-generation therapies targeting complex intracellular environments.

## Acknowledgements

The authors acknowledge funding by the Max Planck-Bristol Centre for Minimal Biology and the Max Planck Society. Oskar Staufer acknowledges the financial support by the Daimler and Benz Foundation (32-12/22), the Joachim Herz Foundation (Add-on Fellowship) and the German Science Foundation (Emmy Noether Program, project number 525255627). This work was supported by the Max Planck Graduate Center (MPGC) with the Johannes Gutenberg University Mainz. Shutian Si and Jana Fetzer acknowledge the financial support from the DFG (Deutsche Forschungsgemeinschaft SFB 1551, project number 464588647).

## Author information

## Authors and Affiliations

**Max Planck Institute for Polymer Research, Mainz, Germany**

Sarah Chagri, Julian Link, Raphael Meyer, Jana Fetzer, Patrick Roth, Yong Ren, Shutian Si, Francesca Mazzotta, Manfred Wagner, Ingo Lieberwirth, Katharina Landfester, David Y.W. Ng, Tanja Weil

**Leibniz Institute for New Materials, Saarbrücken, Germany**

Anna Burgstaller, Oskar Staufer

**Cellular Neurophysiology, Center for Integrative Physiology and Molecular Medicine, Saarland University, Homburg, Germany**

Claudia Schirra

**State Key Laboratory of Chemo/Biosensing and Chemometrics, College of Chemistry and Chemical Engineering, Hunan University, Changsha, PR China**

Zhixuan Zhou

## Contributions

S.C., D.Y.W.N., O.S. and T.W. conceived the project. S.C. performed the synthesis and characterization of peptides and related compounds. S.C. and Z.Z. conducted the LC-MS kinetics analysis. J.L. and P.R. performed dry-state TEM measurements. S.C. and R.M. performed the CD spectroscopy analysis. S.C. conducted the Proteostat aggregation assay. J.L., J.F. and Y.R. aided in the synthesis of control compounds. S.S., F.M., I.L. and K.L. contributed cryo-EM measurements and analysis. S.C. and M.W. performed NMR analysis. A.B. performed RT-DC measurements. O.S. performed cell uptake experiments, imaging via CLSM, cytotoxicity assays and proteome profiler analysis. C.S. performed the CLEM experiments and analysis. D.Y.W.N., O.S. and T.W. supervised the project. All authors have read and approved the final manuscript.

# References


1 Alberts, B. *et al. Molecular Biology of the Cell*. 6. edn, (W. W. Norton & Company, 2014).

2 Zhan, P., Jahnke, K., Liu, N. & Göpfrich, K. Functional DNA-based cytoskeletons for synthetic cells. *Nat. Chem.* **14**, 958–963 (2022).

3 Chagri, S., Ng, D. Y. W. & Weil, T. Designing bioresponsive nanomaterials for intracellular self-assembly. *Nat. Rev. Chem.* **6**, 320-338 (2022).

4 Deng, Y., Zhan, W. & Liang, G. Intracellular Self-Assembly of Peptide Conjugates for Tumor Imaging and Therapy. *Adv. Healthcare Mater.* **10**, 2001211 (2021).

5 Guo, R.-C. *et al.* Recent progress of therapeutic peptide based nanomaterials: from synthesis and self-assembly to cancer treatment. *Biomater. Sci.* **8**, 6175–6189 (2020).

6 Pieszka, M. *et al.* Controlled Supramolecular Assembly inside Living Cells by Sequential Multi-staged Chemical Reactions. *J. Am. Chem. Soc.* **142**, 15780-15789 (2020).

7 Zhou, Z. *et al.* In Situ Assembly of Platinum(II)-Metallopeptide Nanostructures Disrupts Energy Homeostasis and Cellular Metabolism. *J. Am. Chem. Soc.* **144**, 12219–12228 (2022).

8 Ren, Y. *et al.* Supramolecular Assembly in Live Cells Mapped by Real-Time Phasor-Fluorescence Lifetime Imaging. *J. Am. Chem. Soc.* **146**, 11991–11999 (2024).

9 Chen, Z., Chen, M., Zhou, K. & Rao, J. Pre-targeted Imaging of Protease Activity through In Situ Assembly of Nanoparticles. *Angew. Chem. Int. Ed.* **59**, 7864–7870 (2020).

10 Zheng, R. *et al.* Controllable Self-Assembly of Peptide-Cyanine Conjugates In Vivo as Fine-Tunable Theranostics. *Angew. Chem. Int. Ed.* **60**, 7809 –7819 (2021).

11 Raskov, H., Orhan, A., Christensen, J. P. & Gögenur, I. Cytotoxic CD8+ T cells in cancer and cancer immunotherapy. *Br. J. Cancer* **124**, 359–367 (2021).

12 Hwang, J.-R., Byeon, Y., Kim, D. & Park, S.-G. Recent insights of T cell receptor-mediated signaling pathways for T cell activation and development. *Exp. Mol. Med.* **52**, 750–761 (2020).

13 Basu, R. *et al.* Cytotoxic T Cells Use Mechanical Force to Potentiate Target Cell Killing. *Cell* **165**, 100–110 (2016).

14 Waldman, A. D., Fritz, J. M. & Lenardo, M. J. A guide to cancer immunotherapy: from T cell basic science to clinical practice. *Nat. Rev. Immunol.* **20**, 651–668 (2020).

15 Rosenberg, S. A. & Restifo, N. P. Adoptive cell transfer as personalized immunotherapy for human cancer. *Science* **348**, 62–68 (2015).

16 Sahin, U. & Türeci, Ö. Personalized vaccines for cancer immunotherapy. *Science* **359**, 1355–1360 (2018).

17 Goldberg, M. S. Improving cancer immunotherapy through nanotechnology. *Nat. Rev. Cancer* **19**, 587–602 (2019).

18 Göpfrich, K., Platten, M., Frischknecht, F. & Fackler, O. T. Bottom-up synthetic immunology. *Nat. Nanotechnol.* (2024).

19 Quinn, J. F., Whittaker, M. R. & Davis, T. P. Glutathione responsive polymers and their application in drug delivery systems. *Polym. Chem.* **8**, 97–126 (2016).

20 Rashida Gnanaprakasam, J. N., Wu, R. & Wang, R. Metabolic Reprogramming in Modulating T Cell Reactive Oxygen Species Generation and Antioxidant Capacity. *Front. Immunol.* **9**, 342242 (2018).

21 Mak, T. W. *et al.* Glutathione Primes T Cell Metabolism for Inflammation. *Immunity* **46**, 675–689 (2017).

22 Franchina, D. G., Dostert, C. & Brenner, D. Reactive Oxygen Species: Involvement in T Cell Signaling and Metabolism. *Trends Immunol.* **39**, 489–502 (2018).

23 Lian, G. *et al.* Glutathione de novo synthesis but not recycling process coordinates with glutamine catabolism to control redox homeostasis and directs murine T cell differentiation. *eLife* (2018).

24 Estrela, J. M., Ortega, A. & Obrador, E. Glutathione in Cancer Biology and Therapy. *Crit. Rev. Clin. Lab. Sci.* **43**, 143–181 (2006).

25 Smith, D. K. Lost in translation? Chirality effects in the self-assembly of nanostructured gel-phase materials. *Chem. Soc. Rev.* **38**, 684–694 (2009).
26 Tao, K., Levin, A., Adler-Abramovich, L. & Gazit, E. Fmoc-modified amino acids and short peptides: simple bio-inspired building blocks for the fabrication of functional materials. *Chem. Soc. Rev.* **45**, 3935–3953 (2016).
27 Micsonai, A. *et al.* Accurate secondary structure prediction and fold recognition for circular dichroism spectroscopy. *Proc. Natl. Acad. Sci. U.S.A.* **112**, E3095–E3103 (2015).
28 Roth, P. *et al.* Supramolecular assembly guided by photolytic redox cycling. *Nat. Synth.* **2**, 980–988 (2023).
29 Rossy, J., Laufer, J. M. & Legler, D. F. Role of Mechanotransduction and Tension in T Cell Function. *Front. Immunol.* **9** (2018).
30 Gomez, T. S. & Billadeau, D. D. in *Advances in Immunology* Vol. 97 1–64 (Academic Press, 2008).
31 Xue, L., Chiang, L., Kang, C. & Winoto, A. The role of the PI3K-AKT kinase pathway in T-cell development beyond the β checkpoint. *Eur. J. Immunol.* **38**, 3200–3207 (2008).
32 Cantrell, D. Protein kinase B (Akt) regulation and function in T lymphocytes. *Semin. Immunol.* **14**, 19–26 (2002).
33 Kim, E. H. & Suresh, M. Role of PI3K/Akt signaling in memory CD8 T cell differentiation. *Front. Immunol.* **4**, 39750 (2013).
34 Macintyre, A. N. *et al.* Protein kinase B controls transcriptional programs that direct cytotoxic T cell fate but is dispensable for T cell metabolism. *Immunity* **34**, 224–236 (2011).
35 Hussein, M. S., Li, Q., Mao, R., Peng, Y. & He, Y. TCR T cells overexpressing c-Jun have better functionality with improved tumor infiltration and persistence in hepatocellular carcinoma. *Front. Immunol.* **14**, 1114770 (2023).
36 Lynn, R. C. *et al.* c-Jun overexpression in CAR T cells induces exhaustion resistance. *Nature* **576**, 293–300 (2019).
37 Wen, A. Y., Sakamoto, K. M. & Miller, L. S. The Role of the Transcription Factor CREB in Immune Function. *J. Immunol.* **185**, 6413–6419 (2010).
38 Shah, K., Al-Haidari, A., Sun, J. & Kazi, J. U. T cell receptor (TCR) signaling in health and disease. *Sig. Transduct. Target. Ther.* **6**, 412 (2021).
39 D'Souza, W. N., Chang, C.-F., Fischer, A. M., Li, M. & Hedrick, S. M. The Erk2 MAPK Regulates CD8 T Cell Proliferation and Survival. *J. Immunol.* **181**, 7617–7629 (2008).
40 Behrens, A. *et al.* Jun N-terminal kinase 2 modulates thymocyte apoptosis and T cell activation through c-Jun and nuclear factor of activated T cell (NF-AT). *Proc. Natl. Acad. Sci. U.S.A.* **98**, 1769–1774 (2001).